



# Effective Therapeutic Drug Delivery by GALA3, an Endosomal Escape Peptide with Reduced Hydrophobicity

Chen Li<sup>1</sup> · Xue-Wei Cao<sup>1</sup> · Jian Zhao<sup>1,5</sup> · Fu-Jun Wang<sup>2,3,4</sup>

Received: 4 December 2019 / Accepted: 20 January 2020  
© Springer Science+Business Media, LLC, part of Springer Nature 2020

## Abstract

Endosomal escape is a rate-limiting step in the cytosolic delivery of therapeutic drugs. Overcoming this barrier is crucial to achieve an effective biological based therapy. In this work, we evaluated the ability of a synthetic biomimetic peptide derived from the GALA to facilitate endosomal escape of protein drugs. Our results showed that the cytoplasmic distribution of GALA fusion proteins changed according to the hydrophobicity of GALA. One of the synthetic peptides, GALA3, significantly enhanced the endosomal escape efficiency of protein drugs. The cytosolic delivery capacity of GALA3 was significantly higher than that of several previously reported endosomal escape peptides, including hemagglutinin 2 (HA2). Moreover, when GALA3 was fused to BLF1–HBP, a ribosome-inactivating protein with cell-penetrating peptide HBP, the cytotoxicity of the fusion protein was significantly increased in various cell lines, including H460, HeLa, A549, and SMCC-7721. The growth inhibition effect of GALA3–BLF1–HBP was at least 20 times greater than that of BLF1–HBP alone in different tumor cell lines. GALA3 effectively promoted the endosomal escape of BLF1–HBP in a pH-dependent manner and greatly enhanced the apoptotic activity of BLF1–HBP. Taken together, our data show that by adjusting the hydrophobicity of GALA we obtained a more effective endosomal escape peptide. Therefore, GALA3-fusions can improve the efficiency of therapeutic protein drugs.

**Keywords** Endosomal escape · HBP · GALA3 · BLF1

**Electronic supplementary material** The online version of this article (<https://doi.org/10.1007/s00232-020-00109-2>) contains supplementary material, which is available to authorized users.

✉ Jian Zhao  
zhaojian@ecust.edu.cn

✉ Fu-Jun Wang  
wfj@shutcm.edu.cnmail

- <sup>1</sup> State Key Laboratory of Bioreactor Engineering, East China University of Science and Technology, Shanghai, People's Republic of China
- <sup>2</sup> New Drug R&D Center, Zhejiang Fonow Medicine Co., Ltd., 209 West Hulian Road, Dongyang 322100, Zhejiang, People's Republic of China
- <sup>3</sup> Shanghai R&D Center for Standardization of Chinese Medicines, 1200 Cailun Road, Shanghai 201203, People's Republic of China
- <sup>4</sup> Institute of Chinese Materia Medica, Shanghai University of Traditional Chinese Medicine, 1200 Cailun Road, Shanghai 201203, People's Republic of China
- <sup>5</sup> Department of Applied Biology, East China University of Science and Technology, 130 Meilong Road, Shanghai 200237, People's Republic of China

## Introduction

Bioactive macromolecules such as proteins, DNA, and siRNA have great potential for cancer therapy in terms of selectivity and high potency towards their targets. However, the low membrane permeability of these macromolecules greatly limits their therapeutic potency (Fei et al. 2014). With the help of various drug delivery technologies, especially cell-penetrating peptides (CPPs), great progress has been made in the application of bioactive macromolecules (LeCher et al. 2017). Studies have shown that CPPs effectively promote the internalization of cell membrane-impenetrable molecules via endocytosis, including macropinocytosis, caveolin-dependent, clathrin-dependent, and clathrin/caveolin-independent endocytosis (Fonseca et al. 2009; Liou et al. 2012). Unfortunately, efficient endocytosis alone is not sufficient because only negligible fractions of these proteins are released from the endocytic vesicle into the cytosol to exert their bioactivity. In fact, most endocytosed proteins remain trapped in endosomes and will eventually be degraded in lysosomes (Andersson et al. 2009; Brock

et al. 2018; Salomone et al. 2012). To improve the efficacy of protein drugs, it is crucial to find effective methods to promote their cytosolic delivery.

Various methods have been reported to improve endosomal escape efficiency (Erazo-Oliveras et al. 2012, 2014; Fuchs et al. 2013). HA2, a small peptide derived from the major envelope glycoprotein of human influenza virus, has been used as a canonical endosomal escape peptide (EEP) in several studies (El-Sayed et al. 2009; Esbjorn et al. 2007; Golan et al. 2016; Liou et al. 2012). In the low pH environment characterizing the evolution of the late endosome into a lysosome, HA2 adopts a stable helical structure, which forms a pore structure in the endosomal membrane, allowing the release of the contents of the endosome into the cytosol (Cross et al. 2009; Varkouhi et al. 2011; Wang et al. 2010a, b). Other EEPs (also known as fusogenic peptides), including gp41 and gph, among others, act in a similar way to release protein drugs from the endosomes into the cytosol (Varkouhi et al. 2011).

Recently, a number of synthetic analogues of natural EEPs have attracted much attention (Varkouhi et al. 2011). Compared to EEPs isolated and derived from natural sources, these peptides have many advantages, including a specific sequence, hydrophobicity and a flexible length (Shete et al. 2014; Varkouhi et al. 2011). GALA is a synthetic amphipathic peptide derived from a mutant sequence of HA2 with a substitution of glycine by glutamic acid at position 4. GALA contains 30 amino acids with a repeat sequence consisting of glutamic acid–alanine–leucine–alanine (EALA), an N-terminal tryptophan, and including a histidine residue (Li et al. 2004). The  $\alpha$ -helical conformation of GALA, driven by the protonated Glu residues at pH 5, displays membrane fusogenic activity (Hatakeyama et al. 2009; Li et al. 2004). Application of GALA in cationic liposomes and nanocarriers to deliver drugs or nucleic acids has shown a remarkable membrane-disruptive property (Futaki et al. 2005; Locke and Sofou 2017; Sasaki et al. 2008). However, the effect of GALA on the endosomal escape of protein drugs is still unknown.

We previously have shown that HBP, a highly efficient CPP derived from the heparin-binding domain of heparin-binding epidermal growth factor-like growth factor (HB-EGF) (Luo et al. 2016), increased the membrane transport efficiency of the fusion protein by 300-fold when it was fused to the enhanced green fluorescent protein (EGFP). However, unexpectedly, when HBP was fused to BLF1 (*Burkholderia* lethal factor 1) (Hautbergue and Wilson 2012), a ribosome-inactivating protein (RIP) isolated from *Burkholderia pseudomallei*, the cytotoxicity of BLF1–HBP was only 3.38 times higher than that of BLF1 alone ( $IC_{50}$  for BLF1–HBP was 14,965 nM, whereas  $IC_{50}$  for BLF1 alone was 50,607 nM) (Fig. S1). Similar results were observed when HBP was fused with MAP30 (*Momordica Antiviral*

*Protein* 30 kDa), another RIP with a different structure and features (Luo et al. 2016; Meng et al. 2012). This improvement effect is much lower than the previous example of EGFP fusion protein. It is speculated that most endocytic protein drugs may still be trapped in endosomes and cannot be effectively released to the target site to exert their bio-activities. In our preliminary study, GALA was fused with EGFP–HBP to promote the endosomal escape efficiency of the fusion protein. However, the introduction of GALA not only failed to improve the endosomal escape efficiency of EGFP–HBP, but actually reduced the intracellular delivery of the fusion proteins. It has been proposed that peptides with higher hydrophobicity easily self-associate and aggregate on the plasma membrane, which may hinder transmembrane delivery (Dathe and Wieprecht 1999; Verdurmen et al. 2013; Wang et al. 2010a, b). Therefore, we speculated that the presence of GALA caused the fusion protein to aggregate on the cell membrane due to hydrophobicity issues. Rationally reducing the repeating unit of GALA sequence (EALA) might alleviate this effect while still retaining endosomal escape activity.

In this study, we gradually reduced the number of repeating units of EALA in GALA to lower its hydrophobicity, thereby developing EEPs with high efficiency of endosomal escape. Using this strategy, we successfully constructed a novel peptide named GALA3, which significantly increased the endosomal escape efficiency of a BLF1 fusion protein, resulting in improved growth inhibition of tumor cells.

## Materials and Methods

### Construction of Plasmids

The prokaryotic expression plasmids GALA–EGFP–HBP–pET28a, GALA $_n$ –EGFP–HBP–pET28a ( $n = 1, 2, 3, 4$ ), HA2–EGFP–HBP–pET28a, gph–EGFP–HBP–pET28a, Aurein–EGFP–HBP–pET28a, and vGALA3–EGFP–HBP–pET28a were all synthesized by Genaray Corporation (Shanghai, China). Plasmids EGFP–HBP–pET28a, BLF1–HBP–pET28b, BLF1–pET28b, MAP30–HBP–pET28b were stored in our laboratory. The MAP30 and BLF1 cDNA sequences were cloned from MAP30–HBP–pET28b and BLF1–HBP–pET28b, respectively, and inserted between Nde I and BamH I restriction sites in the GALA3–EGFP–HBP–pET28a plasmid, termed GALA3–MAP30–HBP–pET28a and GALA3–BLF1–HBP–pET28a plasmid, respectively.

### Expression and Purification of Recombinant Protein

Plasmids were transformed into *Escherichia coli* BL21 (DE3) competent cells. Primary cultures were amplified

in fresh Luria Bertani (LB) medium (30 mL) containing kanamycin (50 µg/mL) at 37 °C for 13 h. Then, 4 mL of primary culture was inoculated into LB medium (200 mL) containing kanamycin (50 µg/mL) at 37 °C for 2–3 h. Next, isopropyl- $\beta$ -D-1-thiogalactopyranoside (IPTG, 0.5 mM) (Sangon Biotech, Shanghai) was added when the OD<sub>600</sub> reached 0.6–0.8. Cells were incubated for 16 h at 16 °C and subsequently harvested by centrifugation (3000×g, 20 min) at room temperature. Cells were resuspended in Tris–HCl buffer (20 mM Tris–HCl, 0.5 M NaCl, 5% glycerol, pH 8.5), followed by sonication. The supernatants containing the recombinant proteins were collected by centrifugation (12,000×g, 20 min, 4 °C). The proteins were purified by Ni–NTA affinity chromatography according to a standard protocol. Next, the proteins were dialyzed against dialysis buffer (20 mM Tris–HCl, 0.5 M NaCl, 5% glycerol, pH 7.2). Protein concentrations were evaluated using the BCA assay and the proteins were stored at – 80 °C.

### Cell Culture

Tumor cell lines including H460 (human lung carcinoma), HeLa (human cervical cancer cell), A549 (human non-small cell lung cancer cell) and SMMC-7721 (human hepatic cancer cell, referred to as SMMC) were purchased from the Institute of Biochemistry and Cell Biology, Chinese Academy of Sciences (Shanghai, China). All cell lines were cultured in RPMI-1640 (HyClone, South Logan, Utah, USA) supplemented with 10% fetal bovine serum (FBS) (GEM-INI), streptomycin (100 U/mL), and penicillin (100 U/mL) at 37 °C in 5% (v/v) CO<sub>2</sub>.

### Confocal and Fluorescence Microscopy

Tumor cells (1.0×10<sup>4</sup> cells per well) were seeded in 24-well plates (Corning, NY, USA) and incubated at 37 °C overnight until 30% confluency. The tumor cells were treated with recombinant proteins at the indicated concentrations. After incubation for 12 h, the cells were washed three times with precooled PBS (2.7 mM KCl, 137 mM NaCl, 10 mM Na<sub>2</sub>HPO<sub>4</sub>, and 2 mM KH<sub>2</sub>PO<sub>4</sub>), fixed with paraformaldehyde (PFA, 4%) (Sangon, Shanghai, China), and stained with 4,6-diamidino-2-phenylindole (DAPI) (Beyotime, Haimen, China) in the dark. For lysosome colocalization studies, Lyso-Tracker Red (Beyotime, Haimen, China) was added to the culture medium prior to washing with PBS. The intracellular fluorescence distribution of recombinant proteins was imaged by confocal laser scanning microscopy (CLSM) (Nikon, Tokyo, Japan) and fluorescence microscopy (Nikon, Tokyo, Japan), and the data were analyzed using NLS software (Nikon Co. Ltd., Tokyo, Japan).

### Flow Cytometry

Tumor cells were seeded in 6-well plates (Corning, NY, USA) at a density of 1×10<sup>6</sup> cells per well and cultured overnight. The culture medium was replaced with fresh culture medium containing recombinant proteins at the indicated concentrations. Following incubation, the cells were treated with trypsin, washed twice with PBS, collected, and finally resuspended in PBS. The fluorescence intensity was assessed using flow cytometry (Becton Dickinson, Franklin Lakes, NJ, USA). Data were analyzed using FlowJo 7.6 software (TreeStar, Ashland, Oregon, USA).

### Cell Viability Assay

The growth promotion effects of recombinant proteins were determined *in vitro* using the 3-(4,5-dimethyl-2-thiazolyl)-2,5-diphenyl-2-H-tetrazolium bromide (MTT) assay. Cells (4×10<sup>3</sup> cells per well) were seeded in 96-well plates (Corning, NY, USA), grown to 60% confluence, followed by treatment with fusion proteins at different concentrations for 48 h. Next, 20 µL of MTT (5 mg/mL) (Sango, Shanghai, China) solution were added per well and incubation was continued at 37 °C for 3 h. Then, the culture medium was replaced with 150 µL of dimethyl sulfoxide (DMSO) (Lingfeng, Shanghai, China). The absorbance of each well (OD<sub>492</sub>) was detected using a microplate reader (Thermo Scientific, Waltham, MA).

To further analyze the mechanism by which GALA3 promotes endosomal escape, HeLa cells (4×10<sup>3</sup> cells per well) were seeded in 96-well plates and incubated at 37 °C overnight. Then, recombinant proteins at different concentrations were added in the absence or presence of bafilomycin A1 (50 nM) or monensin (5 µM) and incubated for 48 h. Cell viability was assessed using an MTT assay as described above.

### Hemolysis Assay

The hemocompatibility of GALA3 was evaluated by hemolysis assay. Fresh blood was obtained from the eye of a mouse. Erythrocytes were collected by centrifugation at 4000 rpm for 5 min, washed twice with PBS (1 mL), and finally resuspended in 3 mL PBS. Recombinant proteins (10 µM) were added to the resuspended erythrocytes (200 µL) followed by incubation for 2 h at 37 °C. The samples were centrifuged at 4000 rpm for 10 min, and the absorbance (OD 540) of each sample was detected using a microplate reader. The recombinant protein was replaced with PBS or ddH<sub>2</sub>O as the negative or positive control, respectively.

## Apoptosis Assay

The PE Annexin V Apoptosis Detection Kit with 7-AAD (Sony Biotechnology, Tokyo, Japan) was used to analyze cellular apoptosis. Cells ( $1.0 \times 10^6$  cells per well) were seeded in 6-well plates and cultured until reaching 60% confluence. The culture medium was replaced with fresh medium containing various recombinant proteins for 24 h. Next, cells were rinsed three times with precooled PBS and trypsinized as described above. Subsequently, the resuspended cells were analyzed by flow cytometry (Becton Dickinson, New Jersey, USA).

## Assessment of Topological Inactivation Activity

Ribosome-inactivating proteins have a topological inactivation activity and can cleave supercoiled double-stranded

DNA (S) into linear bands (L) or nicked bands (N). GALA3–MAP30–HBP and MAP30–HBP ( $1 \mu\text{g}/\mu\text{L}$ ) were added to a reaction mixture ( $20 \mu\text{L}$ ) containing  $1 \mu\text{g}$  plasmid,  $100 \text{ mM}$   $\text{MgCl}_2$ ,  $100 \text{ mM}$  KCl and  $20 \text{ mM}$  Tris–HCl (pH 8.5). After incubation in  $37 \text{ }^\circ\text{C}$  for 4 h, the plasmid samples were separated by 1.0% agarose gel electrophoresis and visualized using a gel imaging system (Tanon, Shanghai).

## Statistical Analysis

All data were obtained from at least three independent experiments and are expressed as the means  $\pm$  SEM. Student's t test was used to identify significance, and statistical significance was defined as  $P < 0.05$ .

**Fig. 1** Analysis of the intracellular delivery efficiency of the GALA fusion protein. **a** HeLa cells were incubated with different concentrations (0.125, 0.25, and  $1 \mu\text{M}$ ) of GALA–EGFP–HBP for 12 h, co-stained with DAPI and observed by fluorescence microscope. **b** HeLa cells were incubated with  $0.5 \mu\text{M}$  of EGFP–HBP or GALA–EGFP–HBP for 12 h. The fluorescence intensity was quantified by flow cytometry. The median values of fluorescence intensity were calculated using FlowJo 7.6 software. Error bars represent the mean  $\pm$  SEM,  $n = 3$ .  $**P < 0.01$ . **c** HeLa cells were incubated with GALA–EGFP–HBP at  $0.2 \mu\text{M}$  for 12 h, and imaged by fluorescence microscopy

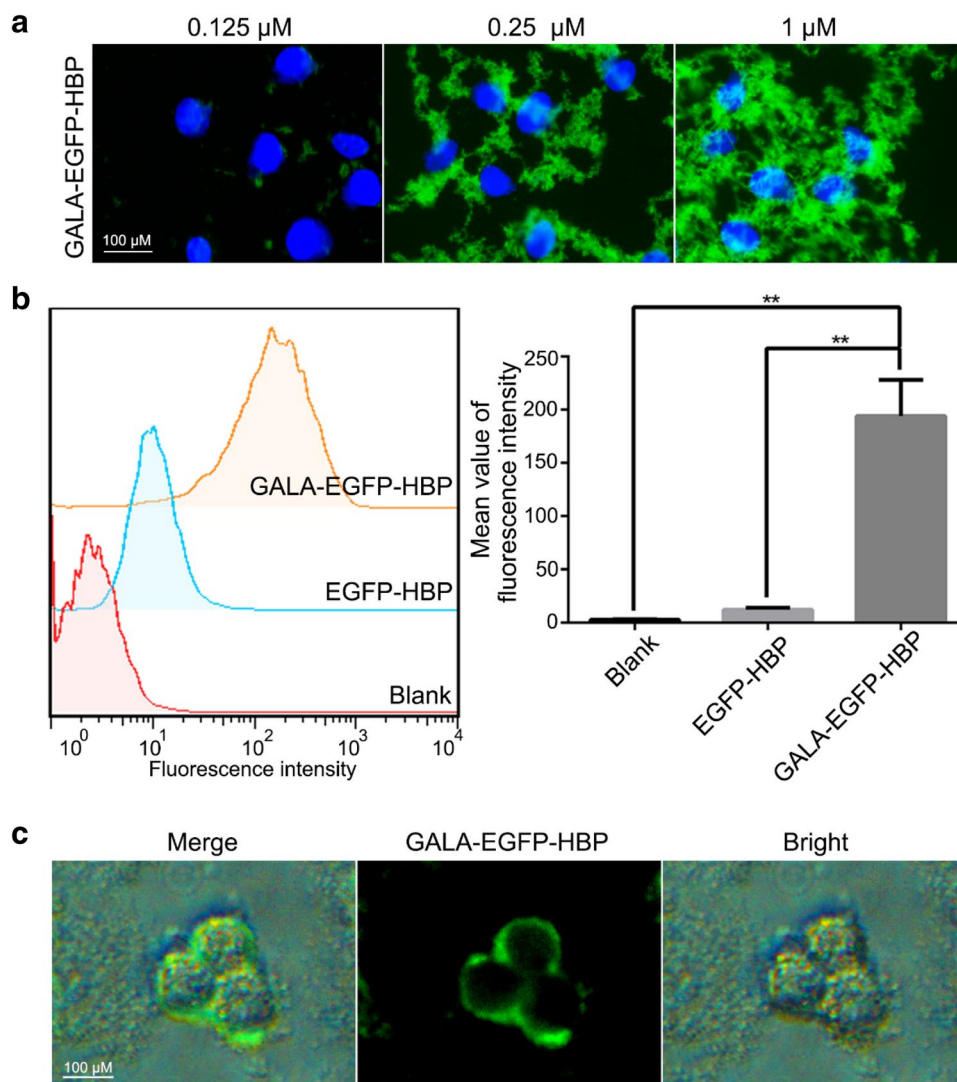


**Table 1** Amino acid sequence of GALA $n$ 

Mutant name	Amino acid sequence
GALA1	LA EALA A
GALA2	LA EAL EALA A
GALA3	LA EALA EAL EALA A
GALA4	LA EALA EALA EAL EALA A
GALA	W EAALA EALA EALA EHLA EALA EAL EALA A

## Results

### Analysis of the Ability of the GALA Peptide to Perform Intracellular Delivery of Fusion Proteins

GALA is a synthetic analogue that mimics the natural EEP HA2 (Li et al. 2004; Subbarao et al. 1987). To observe the distribution of endocytic GALA fusion proteins in our experimental system, EGFP was fused with GALA and HBP. The GALA–EGFP–HBP fusion protein was expressed in bacteria and purified by Ni–NTA chromatography. Next, the GALA–EGFP–HBP fusion protein was added to HeLa cells at different concentrations and its intracellular distribution was observed by fluorescence microscopy. The results showed that GALA–EGFP–HBP was translocated into cells in a dose-dependent manner (Fig. 1a).

Flow cytometry analysis confirmed that GALA significantly enhanced the intracellular delivery efficiency of EGFP–HBP (Fig. 1b).

However, it appeared that most fusion proteins aggregated on the cell membrane at high concentrations. In order to examine its fluorescence distribution, GALA–EGFP–HBP (0.2  $\mu$ M) was incubated with HeLa cells for 12 h. The results

further indicated that GALA–EGFP–HBP appeared to be concentrated on cell membranes and with no green fluorescence in the intracellular region (Fig. 1c). These results indicated that the fluorescence intensity of GALA–EGFP–HBP in HeLa was much higher than of EGFP–HBP, while GALA–EGFP–HBP was mainly aggregated at the cell membrane rather than the cytoplasm.

### Design and Analysis of GALA Mutant Sequence

It has been reported that peptides with high hydrophobicity are prone to self-association and aggregation (Dathe and Wieprecht 1999). In order to solve the problem of aggregation of fusion proteins on the cell membranes, we attempted to reduce the hydrophobicity of the GALA peptide by reducing the number of sequence repeats. The original GALA sequence is mainly composed of EALA repeats. Therefore, we gradually reduced the number of EALA repeats by  $n$  ( $n = 1, 2, 3,$  and  $4$ ). The corresponding deletion mutant peptides were named GALA $n$  ( $n = 1, 2, 3,$  and  $4$ ) (Table. 1).

The crystal structures of GALA and GALA $n$  are displayed in Fig. 2. Furthermore, the helical wheel presentations of GALA and GALA $n$  are given in Fig. 2. The results indicated that the hydrophobic face of GALA $n$  peptides decreased as the number of repeating sequences decreased. Compared with the original GALA, the hydrophilic and hydrophobic distribution of GALA $n$  peptides was more symmetrical and continuous (Fig. 2).

### Intracellular Distribution of GALA $n$ -Fusion Proteins

Theoretical analysis of the structure and hydrophobicity of GALA $n$  peptides showed that the reduction of EALA repeats effectively modulates the distribution of hydrophobic and hydrophilic amino acid residues. To evaluate whether the

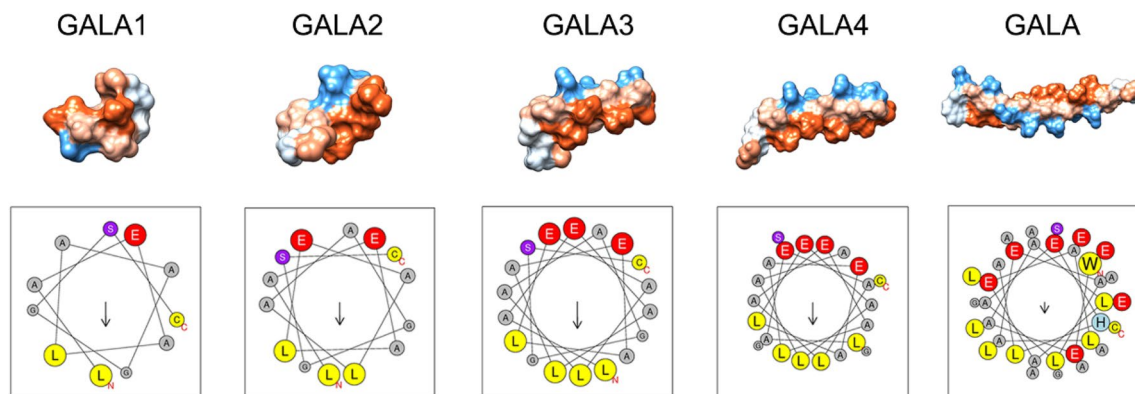


**Fig. 2** Design and analysis of GALA mutant sequence. The structure of GALA and GALA $n$  ( $n = 1, 2, 3,$  and  $4$ ). The cartoon diagram of the crystal structures of the peptides as predicted by Chimera v1.10.2. The hydrophilic domain was showed as blue, and the hydrophobic domain was showed as red. Helical wheel projections for the peptides

were generated using HeliQuest. Yellow circles represent hydrophobic residues, gray circles represent non-polar residues and red circles denote acidic amino acids. Arrows indicate relative hydrophobic moment, a measure of the amphipathicity of peptides in an  $\alpha$ -helical conformation (Color figure online)

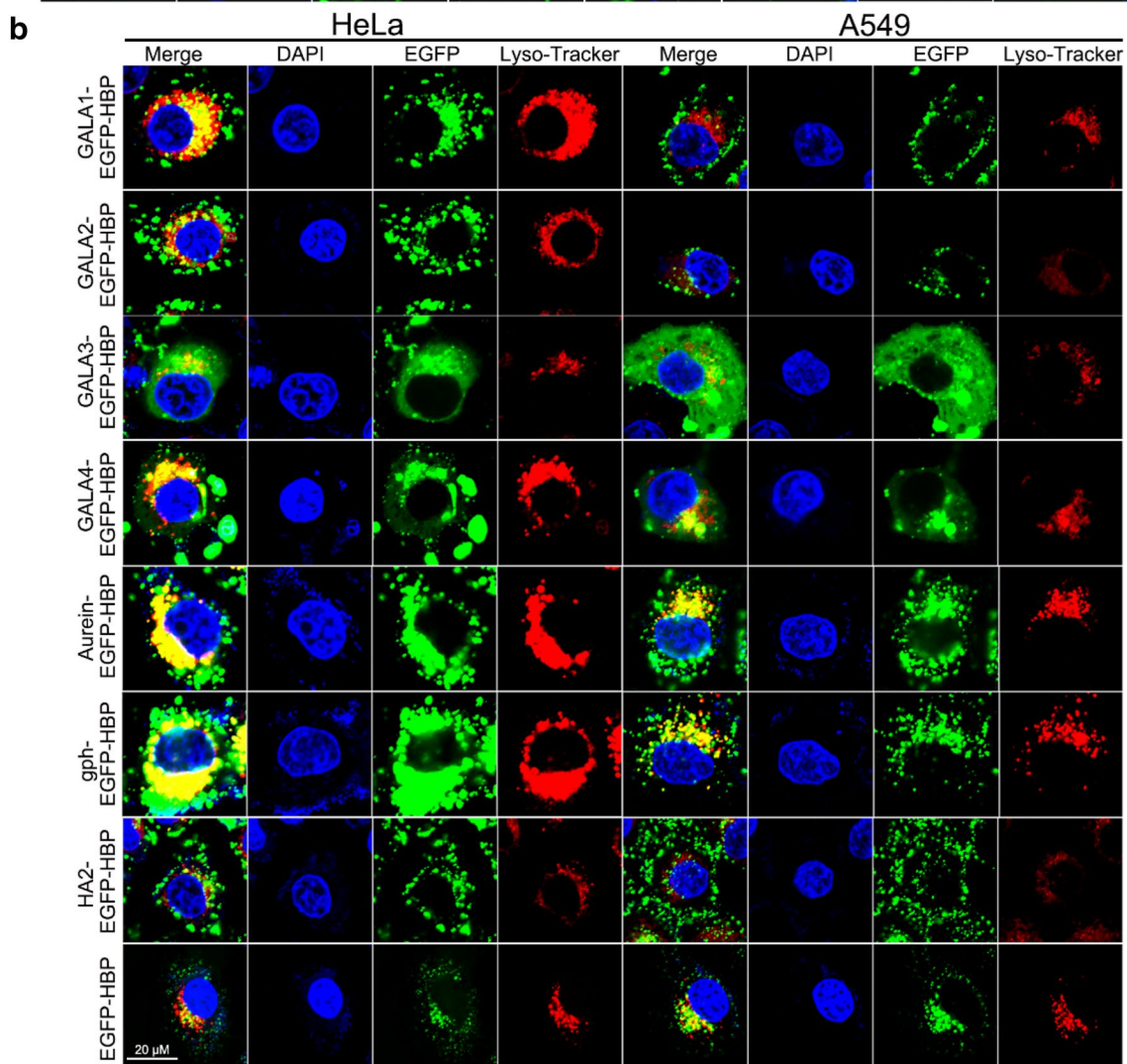
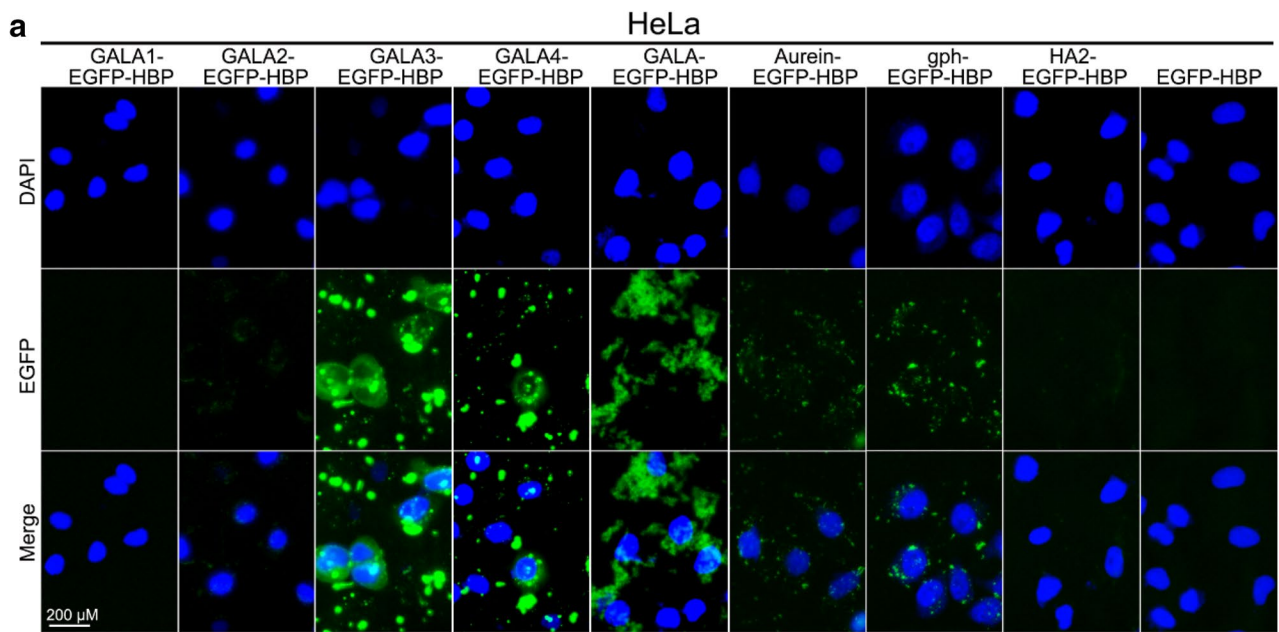


**Fig. 3** Intracellular distribution of GALA $n$ -fusion proteins. **a** HeLa cells were treated in the presence of various fusion proteins at a concentration of 0.25  $\mu$ M for 12 h at 37 °C. The images were captured by a fluorescence microscope and nuclei were stained with DAPI (blue). **b** HeLa cells and A549 cells were treated with GALA1-EGFP-HBP, GALA2-EGFP-HBP, HA2-EGFP-HBP, gph-EGFP-HBP, Aurein-EGFP-HBP, EGFP-HBP (5  $\mu$ M), GALA3-EGFP-HBP, GALA4-EGFP-HBP (0.25  $\mu$ M) for 12 h, co-stained with DAPI and Lyso-Tracker Red, and observed by confocal fluorescence microscopy (Color figure online)

decrease in hydrophobicity seen in GALA $n$  peptides attenuates protein aggregation on the cell membrane and exerts its endosomal escape ability, DNA sequences encoding GALA $n$  peptides were fused with the EGFP-HBP gene sequence, and the resulting plasmids (GALA $n$ -EGFP-HBP-pET28a) were transformed into *E. coli* BL21 (DE3) and expressed. The expressed GALA $n$ -EGFP-HBP fusion proteins were purified by Ni-NTA chromatography. The different GALA $n$ -EGFP-HBP fusion proteins (0.25  $\mu$ M) were incubated with HeLa cells for 12 h at 37 °C, and their intracellular distribution was observed by fluorescence microscopy and compared with the distribution of GALA-EGFP-HBP. Consistent with our previous experimental results, GALA-EGFP-HBP was found substantially aggregated on the cell membrane. Cells incubated with GALA1-EGFP-HBP or GALA2-EGFP-HBP showed no significant fluorescent signal. Those cells co-incubated with GALA4-EGFP-HBP mainly showed a weakly scattered fluorescence distribution, indicating that the endocytic recombinant protein was mainly colocalized with the endosome. Interestingly, however, the intracellular fluorescence HeLa cells co-incubated with the GALA3-EGFP-HBP fusion protein was not only strong but also had a very prominent cytoplasmic dispersion, indicating that a substantial percentage of GALA3-EGFP-HBP fusion proteins escaped from the endosomes to the cytoplasm following endocytosis (Fig. 3a). As a control, fusion proteins of three classical EEPs [HA2 (Golan et al. 2016), gph (Ying and Kim 2008), and Aurein (Ambroggio et al. 2005)] with EGFP-HBP, incubated with HeLa cells at the same concentration of GALA3-EGFP-HBP, showed no significant dispersed cytoplasmic distribution (Fig. 3a). From the above experimental results, we concluded that GALA3 is a promising EPP.

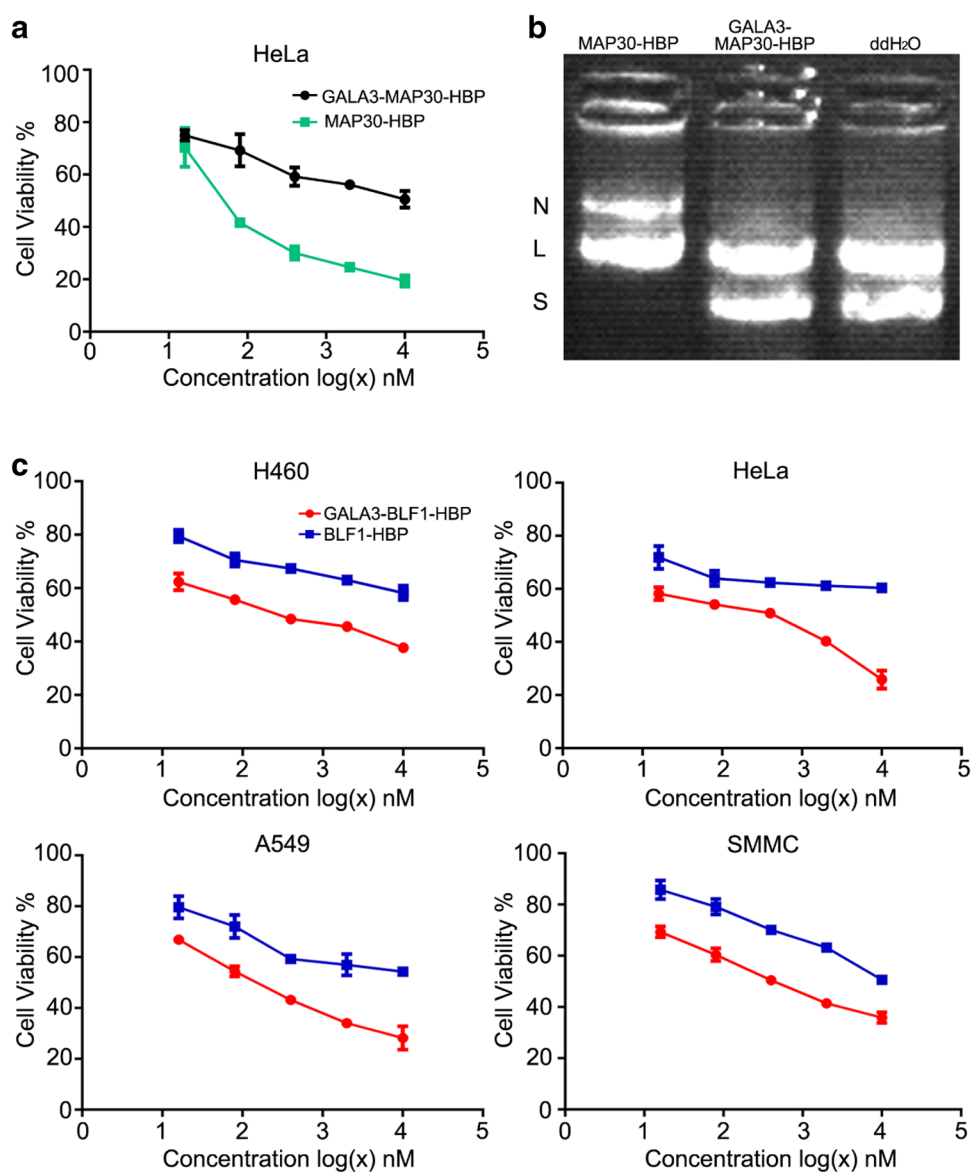
To further investigate the endosomal escape efficiency of GALA $n$ -EGFP-HBP in different cell lines and to assess the colocalization of endocytic fusion proteins and lysosomes, the fusion proteins were incubated with HeLa and A549 cells, respectively. Next, the cells were stained with Lyso-Tracker, a lysosomal marker (red), and then observed with confocal laser scanning microscope (CLSM). The results showed that GALA1-EGFP-HBP and GALA2-EGFP-HBP mainly accumulated in lysosomes and was not released into the cytosol even at higher concentrations (5  $\mu$ M). These

fusion proteins (green) were still distributed in a punctate pattern and highly colocalized with Lyso-Tracker (red) (Fig. 3b). Likewise, GALA4-EGFP-HBP (0.25  $\mu$ M) was also mostly colocalized with Lyso-Tracker and displayed only weak intracellularly dispersed fluorescence. Unlike the above three recombinant proteins, GALA3 significantly promoted the escape of EGFP-HBP from endosomes to the cytoplasm, showing that the GALA3-EGFP-HBP fusion protein (0.25  $\mu$ M) diffused from the punctate vacuoles and was no longer colocalized with the Lyso-Tracker (Fig. 3b). In contrast, HA2-EGFP-HBP, gph-EGFP-HBP, and Aurein-EGFP-HBP showed no apparent scattered fluorescence distribution in the cytoplasm, even at higher concentrations (5  $\mu$ M), and these fusion proteins appeared in a punctate pattern in the cells which was highly colocalized with Lyso-Tracker red (Fig. 3b). Therefore, the colocalization experiment demonstrated that GALA3 enhanced the endosomal escape efficiency of GALA3 fusion proteins, and this effect was similar pattern in both HeLa and A549 cell lines, suggesting the universality of this effect.

### GALA3 Enhanced the Intracellular Activity of Endocytic Fusion Proteins in Different Cell Lines

The above results demonstrated the excellent endosomal escape efficiency of GALA3. Subsequently, we fused GALA3 with antitumor protein drugs to test whether the introduction of GALA3 could promote their therapeutic efficiency. Initially, MAP30 (Puri et al. 2012), a RIP which has been reported to have antitumor activity, was used to verify the effect of GALA3. We previously demonstrated that a MAP30-HBP fusion displayed an enhanced antitumor effect compared with MAP30 alone (Luo et al. 2016). We next expressed and purified GALA3-MAP30-HBP and incubated this fusion protein at different concentrations with HeLa cells for 48 h. However, the introduction of GALA3 unexpectedly reduced the inhibitory effect of MAP30-HBP on tumor cell growth (Fig. 4a). The IC<sub>50</sub> values are given in Table 2. We speculated that the introduction of GALA3 affected the biological activity of MAP30. MAP30 possesses multiple biological activities. We used a previously published topological inactivation cleavage assay of supercoiled double-stranded DNA to test whether GALA3 affects the intrinsic activity of MAP30 (Lee-Huang et al. 1995; Luo et al. 2016). The result showed that while MAP30-HBP cleaved supercoiled double-stranded DNA (S) into linear bands (L) or nicked circular bands (N), GALA3-MAP30-HBP did not cleave any S DNA into other types (L or N) (Fig. 4b). These results suggested that the addition of GALA3 caused the attenuation of the intrinsic bioactivity of MAP30-HBP, which may offset the positive effects of its endosomal escape function.

**Fig. 4** GALA3 enhanced the intracellular activity of endocytic fusion proteins in different cell lines. **a** HeLa cells were incubated with different concentrations of GALA3–MAP30–HBP and MAP30–HBP for 48 h. The inhibition ratio of GALA3–MAP30–HBP and MAP30–HBP was measured by an MTT assay. Each bar represents the mean value of five assays  $\pm$  SEM,  $n = 5$ . **b** Reaction mixture contained plasmid (1  $\mu$ g) and either GALA3–MAP30–HBP or MAP30–HBP at a concentration of 1  $\mu$ g/ $\mu$ L at 37  $^{\circ}$ C for 4 h, and cleavage of the plasmid was detected using 1.0% agarose gel electrophoresis. **c** H460, HeLa, A549, and SMMC cells were incubated with different concentrations of GALA3–BLF1–HBP or BLF1–HBP fusion proteins for 48 h. The inhibition ratio of GALA3–BLF1–HBP and BLF1–HBP on different cells was measured by an MTT assay. Each bar represents the mean value of five assays  $\pm$  SEM,  $n = 5$



We next selected BLF1 (Rust et al. 2018; Walsh et al. 2013), another RIP, with a totally different steric structure from MAP30, to test the role of GALA3. The cytotoxicity of BLF1–HBP was not significantly increased compared with HBP alone, which was due to endosomal trapping of the fusion (Fig. S1). However, as expected, the introduction of GALA3 to the BLF1–HBP fusion protein resulted in a significant enhancement of the cytotoxicity of the BLF1–HBP recombinant protein in all tumor cell lines tested (H460, HeLa, A549, and SMMC) (Fig. 4c). According to the  $IC_{50}$  values (Table 3), the inhibitory effect of GALA3–BLF1–HBP on these tumor cells is greater than that of BLF1–HBP. Taken together, these results suggested that GALA3 promoted the endosomal escape efficiency of

recombinant proteins, but that the introduction of GALA3 may attenuate the activity of recombinant proteins.

### The Effect of GALA3 on Cell Viability

While the above experimental results show that GALA3 enhanced the endosomal escape activity of BLF1–HBP fusogenic peptides may cause cytotoxicity due to their unique disruptive effects on membrane structure. Therefore, we next studied the biocompatibility of GALA3 in a hemolysis experiment. Figure 5a shows that ddH<sub>2</sub>O as the positive control caused up to 100% hemolysis of mouse blood, while the hemolytic activity of GALA3–EGFP–HBP at different concentrations was less than 5%, similar to the negative control (PBS). The result of hemolysis assay indicated that GALA3

**Table 2** IC<sub>50</sub> values of MAP30–HBP and GALA3–MAP30–HBP in HeLa cells

	MAP30–HBP (nM)	GALA3–MAP30–HBP (nM)
IC <sub>50</sub>	68.76 ± 0.862	8551.00 ± 13.427

IC<sub>50</sub> values were calculated using GraphPad Prism 6.0 software

is not toxic to red blood cells. In order to evaluate the in vitro cytotoxicity of GALA3 on nucleated cells, we incubated H460 cells with different concentrations of EGFP–HBP, GALA3–EGFP–HBP, or GALA3–BLF1–HBP recombinant proteins for 48 h and then analyzed the cell viability by MTT assay. As shown in Fig. 5b, GALA3–EGFP–HBP had little inhibitory effect on cell growth, similar to the negative control EGFP–HBP, indicating that GALA3 is not cytotoxic on nucleated cells. Meanwhile, a significant decrease in cell viability was observed after incubation with GALA3–BLF1–HBP as a positive control, since BLF1 is a RIP that is cytotoxic to a variety of cells (Rust et al. 2018). Flow cytometry analysis of cells incubated in the presence of GALA3–BLF1–HBP, GALA3–EGFP–HBP, or EGFP–HBP recombinant proteins yielded similar results (Fig. 5c). Together, these results indicated that GALA3 itself has little inhibitory effect on cell growth.

### Mechanism of GALA3–BLF1–HBP Promoted the Antitumor Effect

When the early endosome becomes a late endosome, the pH in the endosome decreases from 6.5 to 5 (Futaki et al. 2005). GALA can promote endosomal escape at pH 5 (Li et al. 2004). As a mutant of the original GALA, we speculated that the endosomal escape function of GALA3 would likewise be related to the pH of the endosome. To confirm this, we used two types of endosome acidification inhibitors, bafilomycin A1 and monensin (Florey et al. 2015; Fuchs et al. 2016). GALA3–BLF1–HBP was co-treated at different concentrations with bafilomycin A1 (50 nM) or monensin (5 μM) in HeLa cells for 48 h, whereafter the cell viability was analyzed by MTT assay. The results showed that co-treatment with bafilomycin A1 or monensin significantly inhibited the cytotoxicity of GALA3–BLF1–HBP on HeLa

cells (Fig. 6a), indicating that GALA3 requires a low pH value to promote endosomal escape, similar to GALA.

It has been reported that BLF1 exerts its cytotoxicity through the induction of cell apoptosis (Rust et al. 2018). To explore whether GALA3 can enhance the cytotoxicity of BLF1–HBP by promoting its apoptotic activity, apoptosis kit was used to determine the ability of different recombinant proteins to induce apoptosis in various tumor cells. We treated H460, HeLa, A549, and SMMC cells with GALA3–BLF1–HBP or BLF1–HBP at a concentration of 10 μM for 24 h and then subjected the cells to flow cytometry analysis using a PE-7-AAD apoptosis kit. As shown in Fig. 6b, the apoptosis rates induced by GALA3–BLF1–HBP in H460, HeLa, A549, and SMMC were 61.75%, 81.09%, 55.94%, and 89.45%, respectively, which was significantly higher than the apoptosis rates induced by BLF1–HBP in these cell lines (21.18%, 34.06%, 16.65%, and 22.93%, respectively). These results indicate that the presence of GALA3 significantly enhanced BLF1–HBP-induced apoptosis at low pH and thus that GALA3–BLF1–HBP inhibits tumor growth more efficiently than BLF1–HBP.

## Discussion

It is well known that most protein drugs enter the cell through endocytosis but are usually trapped in endosomes or degraded by proteases in lysosomes, preventing them from effectively exerting their biological activities (Zuris et al. 2015). HBP is a highly efficient CPP derived from HB-EGF and is often used for the delivery of antitumor drugs. Previous studies have shown that following the HBP-mediated transmembrane delivery of protein drugs, endocytic fusion proteins (such as EGFP–HBP) are mostly distributed in a punctate pattern and highly colocalized with lysosomes. This indicates that protein drugs fused to HBP are also trapped in the endosome/lysosome and unable to fully exert their activity. Therefore, it is critical to find ways to allow the cargos to escape from the endosome/lysosome system so that they can reach their target sites.

The EEP is a promising tool that can be used to improve the release of protein drugs following endocytosis. In previous reports, HA2, a typical endosomal escape domain

**Table 3** IC<sub>50</sub> values of BLF1–HBP and GALA3–BLF1–HBP in different cell lines

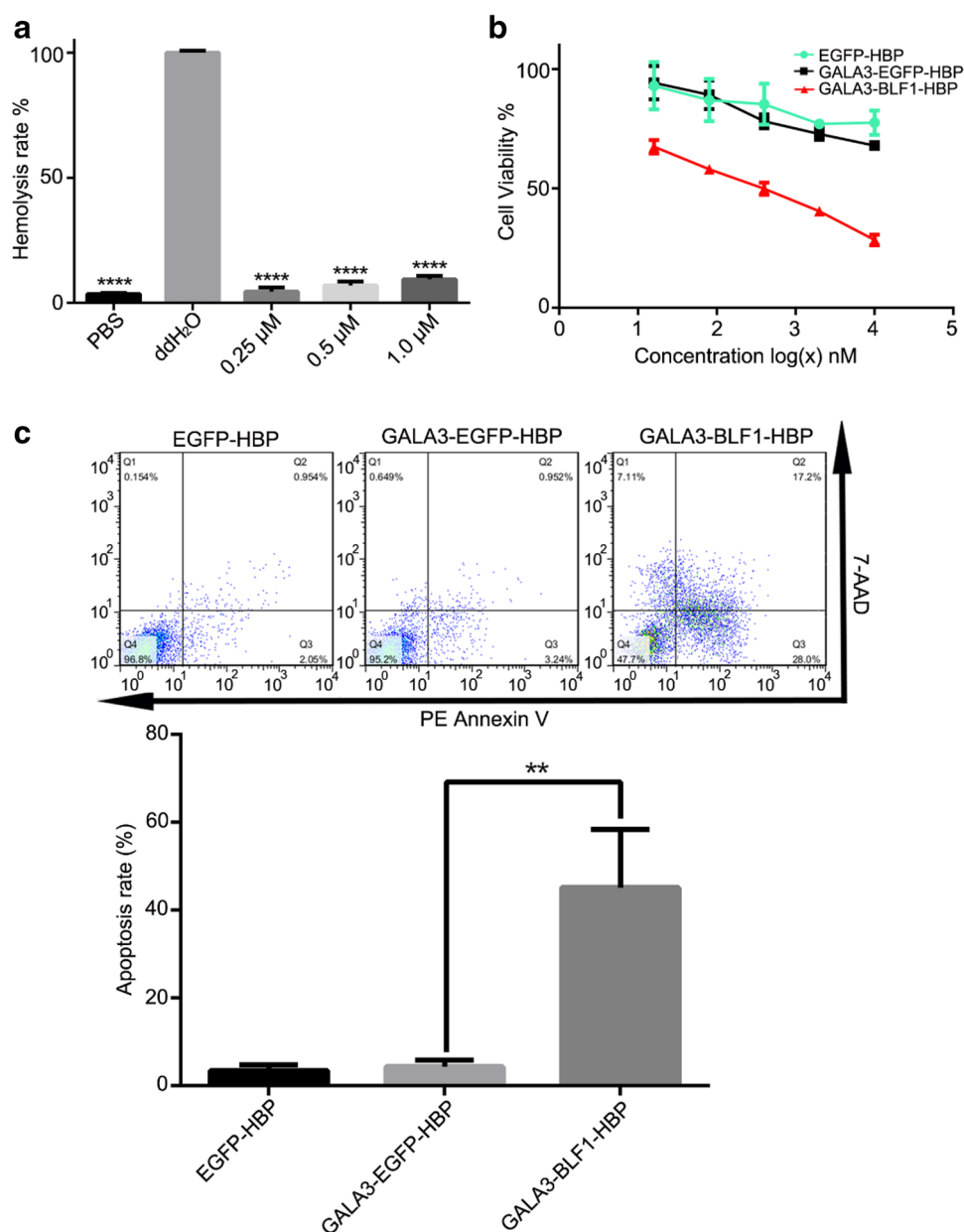
Cell lines	BLF1–HBP (nM)	GALA3–BLF1–HBP (nM)	Fold difference
H460	N/A	396.40 ± 8.359	–
HeLa	N/A	172.60 ± 11.283	–
A549	12,784.00 ± 23.634	179.00 ± 7.531	71.42
SMMC	11,990.00 ± 19.749	529.10 ± 22.214	22.66

IC<sub>50</sub> values were calculated using GraphPad Prism 6.0 software

**Fig. 5** The effect of GALA3 on cell viability. **a** GALA3–EGFP–HBP (10  $\mu$ M) was incubated with mouse blood cells to detect the hemolysis. PBS was used as a negative control and ddH<sub>2</sub>O was used as a positive control. Error bars represent the mean  $\pm$  SEM,  $n=3$ . The difference between positive control and other treated groups is statistically significant, \*\*\*\* $P<0.0001$ .

**b** H460 cells were incubated with different concentrations of EGFP–HBP, GALA3–EGFP–HBP, and GALA3–BLF1–HBP, respectively. Cell viability was measured using the MTT assay. Data were presented as mean  $\pm$  SEM,  $n=5$ .

**c** H460 cells were incubated with EGFP–HBP, GALA3–EGFP–HBP, or GALA3–BLF1–HBP at a concentration of 5  $\mu$ M for 24 h. Cells were collected and stained with 7-AAD and R-phycoerythrin (PE) Annexin V, and then analyzed by flow cytometry. Data were presented as median  $\pm$  SEM,  $n=3$ . Apoptotic rate = late apoptotic rate (Q2) + early apoptotic rate (Q3). \*\* $P<0.01$

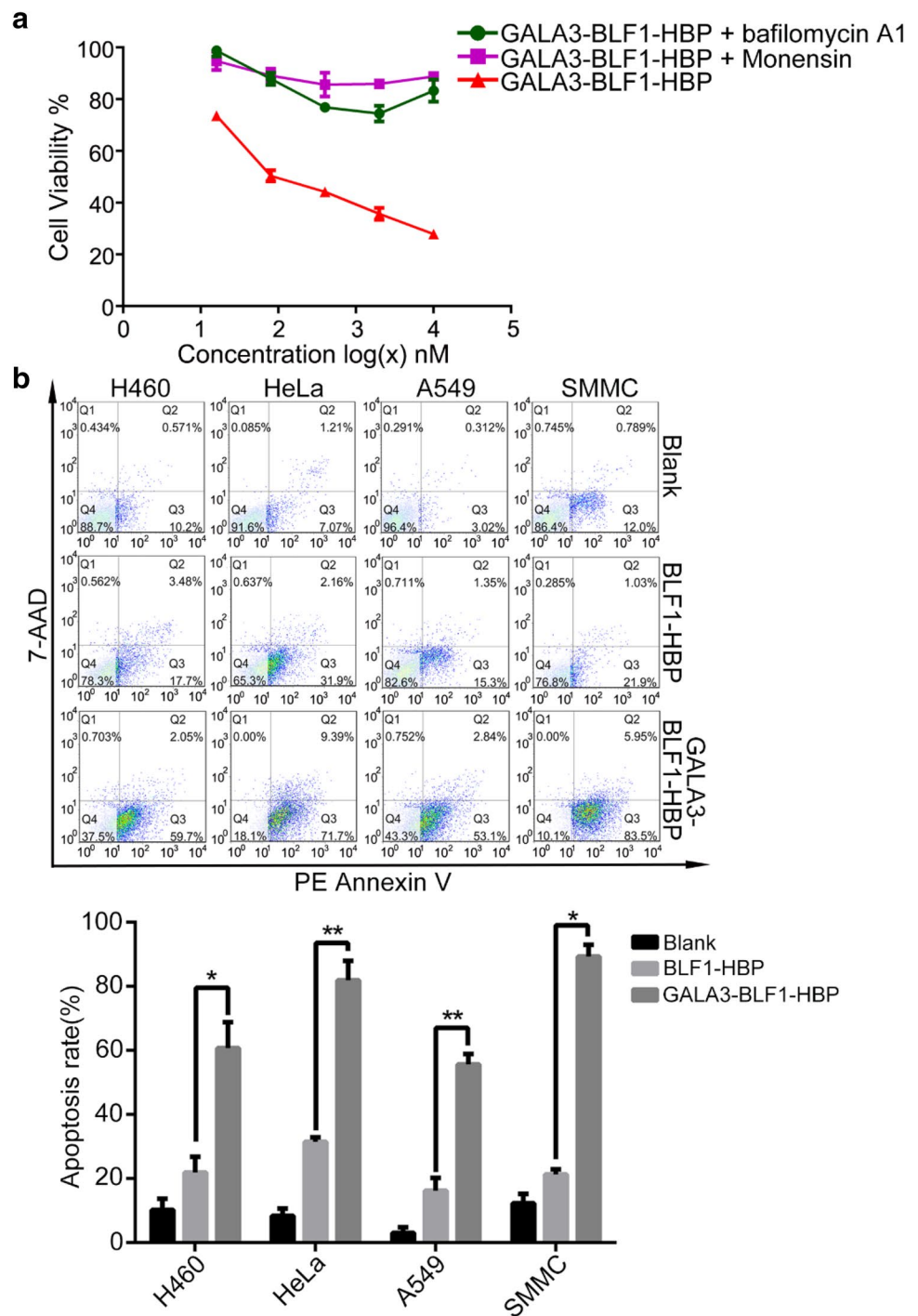


derived from human influenza virus, has been extensively used to promote the escape of various biological macromolecular materials (such as nucleic acids and proteins) from endosomes through membrane fusion (Golan et al. 2016). We therefore attempted to release EGFP–HBP from endosomes by fusion with HA2 but did not achieve satisfactory results. We speculated that the ability of certain peptides to enhance endosomal escape depends on the structural characteristics of the recombinant protein after fusion. For example, the escape efficiency of HA2–R9–mCherry was found to be significantly better compared with R9–mCherry alone (Liou et al. 2012). However, no prominent endosomal escape effect was observed after fusion of HA2 with TAT–EGFP (Cesbron et al. 2015; Patel et al. 2019).

Therefore, we searched for a new EEP to facilitate the escape of recombinant proteins fused to HBP from the endosome.

GALA is a synthetic EEP which promotes the endosomal escape efficiency of small molecules (Futaki et al. 2005; Li et al. 2004). GALA is known to make relatively small pores in model membranes at low concentrations (Wiedman et al. 2014). However, it had been reported that the average pore size induced by GALA3 will increase with increasing GALA:lipid ratio. Under the premise that the GALA concentration is sufficient to release small molecules, when the GALA concentration is continuously increased, a certain number of macromolecules will be released from liposomes (Kuehne and Murphy 2001). GALA had also been shown to transport avidin (68 kDa) to the cytoplasm in the presence

**Fig. 6** GALA3–BLF1–HBP promotes its antitumor effect by inducing apoptosis. **a** HeLa cells were treated with different concentrations of GALA3–BLF1–HBP, in the absence or presence of bafilomycin A1 (50 nM) or monensin (5  $\mu$ M). Cell viability was measured using an MTT assay. Data are presented as mean  $\pm$  SEM,  $n=5$ . **b** H460, HeLa, A549, or SMMC cells were treated with GALA3–BLF1–HBP or BLF1–HBP (10  $\mu$ M) for 24 h. Cells were collected and stained with 7-AAD and PE Annexin V, and then analyzed by flow cytometry. Data are presented as median  $\pm$  SEM,  $n=3$ . Apoptotic rate = late apoptotic rate (Q2) + early apoptotic rate (Q3). \*\* $P < 0.01$ , \* $P < 0.05$



of cationic liposomes (Kobayashi et al. 2009). Therefore, we speculated that the high concentration of GALA might cause the disruption of endosome after forming excessive pores in the endosomal membrane.

GALA modification on liposomes can effectively improve the cytoplasmic transport efficiency of DNA or small molecule drugs. In this study, we investigated whether GALA could be used to promote the endosomal escape efficiency of HBP fusion proteins. GALA is a pH-sensitive endosomal

escape peptide. With the pH decreasing, GALA converts from random coil into a  $\alpha$ -helix (referred to GALA-helix), and the GALA-helix rapidly inserts into the endosomal membrane and assembles into an oligomeric complex, and finally form a circular pore (Roberta et al. 1990). However, while the GALA–EGFP–HBP fusion protein showed significant membrane staining, no fluorescence signal was observed in the cytoplasm, implying poor intracellular delivery efficiency. In contrast, EGFP–HBP without GALA

showed an obvious punctate fluorescence in the cytoplasm, indicating that a significant amount of this fusion protein was successfully translocated into the cells. Some studies have shown that highly hydrophobic proteins tend to aggregate (Martino et al. 2003) and that excessive hydrophobicity will prevent proteins from entering cells, due to protein aggregation or even precipitation (Dathe and Wieprecht 1999; Wang et al. 2010a, b). These proteins aggregate or precipitate on the cell membrane and blocked further cytoplasmic transportation (Wieprecht et al. 1997). In a neutral environment, GALA conformation appears as a random coil, and its binding ability to the cell membrane was greatly affected by hydrophobicity. Therefore, we hypothesized that aggregation of GALA–EGFP–HBP on the cell membrane prevents the fusion protein from entering the cell, due to the strong hydrophobicity of GALA. Thus, we set out to reduce the hydrophobicity of GALA by reducing the number of EALA repeat sequences in the peptide. We were able to select an optimized GALA mutant, GALA3, which endowed HBP fusion proteins with an improved endosomal escape efficiency. To further confirm that the hydrophobicity, rather than peptide length, is a key factor in the aggregation of fusion proteins on cell membranes, we replaced all glutamic acid residues in GALA3 with histidine (since its hydrophobicity is slightly higher than glutamic acid) to increase the hydrophobicity of the peptide but maintain the same peptide chain length (Fig. S2a). This new peptide is denoted as vGALA3. The *grand average of hydropathicity* (GRAVY) was calculated for both vGALA3 and GALA3 by ExPASy (Expert Protein Analysis Software, <https://www.expasy.org/tools/protparam>). The GRAVY value of vGALA3 (1.327) was higher than that of GALA3 (1.236). Consistent with our expectation, GALA3–EGFP–HBP can escape from the endosome to the cytoplasm, but after increasing the hydrophobicity of GALA3 (vGALA3), the vGALA3–EGFP–HBP fusion protein mainly aggregates on the cell membrane, similar to GALA–EGFP–HBP (Fig. S2b). These results proved that the increased hydrophobicity rather than peptide chain length caused aggregation of the fusion protein on the cell membrane. However, considering that GALA3 is only half the length of GALA, the shortening of the length may result in a different structure, net charge, and charge distribution of GALA3. These changes might directly or indirectly affect the endosomal escape activity of GALA3. In subsequent studies, we will further investigate whether the escape ability of GALA3 is affected by these factors.

Interestingly, when GALA3 was fused to two different RIPs, MAP30 and BLF1, the two fusion proteins showed completely different results. GALA3–BLF1–HBP significantly inhibited the growth of tumor cells compared with BLF1–HBP, while the ability of GALA3–MAP30–HBP to inhibit tumor cell growth was even lower than that of MAP30–HBP. Our supercoiled plasmid DNA cleavage

experiments suggested that this abnormality may be due to the introduction of GALA3 affecting the biological activity of MAP30 itself, not necessarily because GALA3 loses its endosomal escape activity. Indeed, the introduction of new domains may affect the activity of the original protein due to steric hindrance. BLF1, a new type of RIP, has a steric structure and bioactivity that is totally different from the typical RIPs (such as MAP30 in this article) (Cruz-Migoni et al. 2011; Walsh et al. 2013). We speculated that the introduction of GALA3 may affect the structure of the cargo protein or block the active site of the cargo protein. However, the different three-dimensional structures of BLF1 and MAP30 caused the very different results presented here. Therefore, although GALA3 is an effective EEP, the successful use of the GALA3 escape activity also requires consideration of its effect on the activity of the original protein.

Our experiments also showed that among various known CPPs, only GALA3 significantly improved the endosomal escape efficiency of EGFP–HBP fusion proteins. When EGFP was fused with other classical CPPs, such as TAT (Fonseca et al. 2009) and R9 (Futaki 2002), only weak punctate distribution of fluorescence was observed within the cell, suggesting either a low delivery efficiency of the fusion protein or the entrapment of the fusion protein in the endosome/lysosome (Fig. S3). Further investigation showed that although HBP, TAT, and R9 are all efficient CPPs, they have different endocytic pathways for bringing cargo into cells. Proteins fused with TAT or R9 are mainly taken up by cells through macropinocytosis (Lonn et al. 2016; Nakase et al. 2009; Wadia et al. 2004). Different from the fate of conventional endosomes in the cell, macropinosomes, a kind of endosome formed during the endocytosis pathway of macropinocytosis, will undergo a process of pH decline, but do not fuse with lysosomes to degrade their inclusions (Conner and Schmid 2003; Meier et al. 2002; Wadia et al. 2004). As an efficient CPP, HBP mainly delivers exogenous proteins into cells through clathrin-mediated endocytosis and caveolin-mediated endocytosis (Luo et al. 2016). The opportunity for endosomal escape will be affected by the endocytosis pathway that brings the fusion protein into the cells due to the different fate of endosomes (Degors et al. 2019). For example, while branched polyethyleneimine (BPEI) polyplexes can enter cells through multiple endocytic pathways, only the uptake of BPEI through caveolin-dependent endocytosis resulted in endosomal escape and productive transfection (Rehman et al. 2011). This suggests that the efficiency of endosomal escape is indeed related to the endocytosis pathway. Therefore, due to the different endocytic pathways of different fusion proteins, GALA3-mediated endosomal escape efficiency is different from that mediated by TAT or R9.

In summary, we constructed a novel EEP, GALA3, which can effectively promote the escape of GALA3-fusion

proteins from endosomes into the cytoplasm. This peptide can significantly improve the cytoplasmic dispersion of EGFP–HBP and improve the antitumor effect of BLF1–HBP. GALA3 is a promising tool for the development of clinical applications allowing of protein drugs to enter cells by clathrin/caveolin-dependent endocytosis.

**Acknowledgements** The authors declare that they have no conflict of interest regarding the conduct or outcomes of this study. This work was supported by the National Natural Science Foundation of China (Grant No. 81571795)

## References

- Ambroggio EE, Separovic F, Bowie JH, Fidelio GD, Bagatolli LA (2005) Direct visualization of membrane leakage induced by the antibiotic peptides: maculatin, citropin, and aurein. *Biophys J* 89:1874–1881. <https://doi.org/10.1529/biophysj.105.066589>
- Andersson Y, Engebraaten O, Fodstad O (2009) Synergistic anti-cancer effects of immunotoxin and cyclosporin in vitro and in vivo. *Br J Cancer* 101:1307–1315. <https://doi.org/10.1038/sj.bjc.6605312>
- Brock DJ, Kustiyan L, Jiang M et al (2018) Efficient cell delivery mediated by lipid-specific endosomal escape of supercharged branched peptides. *Traffic* 19:421–435. <https://doi.org/10.1111/tra.12566>
- Cesbron Y, Shaheen U, Free P, Lvey R (2015) TAT and HA2 facilitate cellular uptake of gold nanoparticles but do not lead to cytosolic localisation. *PLoS ONE* 10:e0121683. <https://doi.org/10.1371/journal.pone.0121683>
- Conner SD, Schmid SL (2003) Regulated portals of entry into the cell. *Nature* 422:37–44. <https://doi.org/10.1038/nature01451>
- Cross KJ, Langley WA, Russell RJ et al (2009) Composition and functions of the influenza fusion peptide. *Protein Pept Lett* 16:766–778. <https://doi.org/10.2174/092986609788681715>
- Cruz-Migoni A, Hautbergue GM, Artymiuk PJ et al (2011) A Burkholderia pseudomallei toxin inhibits helicase activity of translation factor eIF4A. *Science* 334:821–824. <https://doi.org/10.1126/science.1211915>
- Dathe M, Wieprecht T (1999) Structural features of helical antimicrobial peptides: their potential to modulate activity on model membranes and biological cells. *Biochim Biophys Acta* 1462:71–78. [https://doi.org/10.1016/s0005-2736\(99\)00201-1](https://doi.org/10.1016/s0005-2736(99)00201-1)
- Degors IMS, Wang C, Rehman ZU et al (2019) Carriers break barriers in drug delivery: endocytosis and endosomal escape of gene delivery vectors. *Acc Chem Res*. <https://doi.org/10.1021/acs.accounts.9b00177>
- El-Sayed A, Masuda T, Khalil I et al (2009) Enhanced gene expression by a novel stearylated INF7 peptide derivative through fusion independent endosomal escape. *J Control Release* 138:160–167. <https://doi.org/10.1016/j.jconrel.2009.05.018>
- Erazo-Oliveras A, Muthukrishnan N, Baker R et al (2012) Improving the endosomal escape of cell-penetrating peptides and their cargos: strategies and challenges. *Pharmaceuticals (Basel)* 5:1177–1209. <https://doi.org/10.3390/ph5111177>
- Erazo-Oliveras A, Najjar K, Dayani L et al (2014) Protein delivery into live cells by incubation with an endosomolytic agent. *Nat Methods* 11:861–867. <https://doi.org/10.1038/nmeth.2998>
- EsbjoRner EK, Oglecka K, Lincoln P et al (2007) Membrane binding of pH-sensitive influenza fusion peptides. Positioning, configuration, and induced leakage in a lipid vesicle model. *Biochemistry* 46:13490–13504. <https://doi.org/10.1021/bi701075y>
- Fei L, Yap LP, Conti PS et al (2014) Tumor targeting of a cell penetrating peptide by fusing with a pH-sensitive histidine-glutamate co-oligopeptide. *Biomaterials* 35:4082–4087. <https://doi.org/10.1016/j.biomaterials.2014.01.047>
- Florey O, Gammoh N, Kim SE et al (2015) V-ATPase and osmotic imbalances activate endolysosomal LC3 lipidation. *Autophagy* 11:88–99. <https://doi.org/10.4161/15548627.2014.984277>
- Fonseca SB, Pereira MP, Kelley SO (2009) Recent advances in the use of cell-penetrating peptides for medical and biological applications. *Adv Drug Deliv Rev* 61:953–964. <https://doi.org/10.1016/j.addr.2009.06.001>
- Fuchs H, Bachran C, Flavell DJ (2013) Diving through membranes: molecular cunning to enforce the endosomal escape of antibody-targeted anti-tumor toxins. *Antibodies* 2:209–235. <https://doi.org/10.3390/antib2020209>
- Fuchs H, Weng A, Gilabert-Oriol R (2016) Augmenting the efficacy of immunotoxins and other targeted protein toxins by endosomal escape enhancers. *Toxins (Basel)* 8:200. <https://doi.org/10.3390/toxins8070200>
- Futaki S (2002) Arginine-rich peptides: potential for intracellular delivery of macromolecules and the mystery of the translocation mechanisms. *Int J Pharm* 245:1–7. [https://doi.org/10.1016/s0378-5173\(02\)00337-x](https://doi.org/10.1016/s0378-5173(02)00337-x)
- Futaki S, Masui Y, Nakase I et al (2005) Unique features of a pH-sensitive fusogenic peptide that improves the transfection efficiency of cationic liposomes. *J Gene Med* 7:1450–1458. <https://doi.org/10.1002/jgm.796>
- Golan M, Feinshtein V, David A (2016) Conjugates of HA2 with octaarginine-grafted HPMA copolymer offer effective siRNA delivery and gene silencing in cancer cells. *Eur J Pharm Biopharm* 109:103–112. <https://doi.org/10.1016/j.ejpb.2016.09.017>
- Hatakeyama H, Ito E, Akita H et al (2009) A pH-sensitive fusogenic peptide facilitates endosomal escape and greatly enhances the gene silencing of siRNA-containing nanoparticles in vitro and in vivo. *J Control Release* 139:127–132. <https://doi.org/10.1016/j.jconrel.2009.06.008>
- Hautbergue GM, Wilson SA (2012) BLF1, the first Burkholderia pseudomallei toxin, connects inhibition of host protein synthesis with melioidosis. *Biochem Soc Trans* 40:842–845. <https://doi.org/10.1042/BST20120057>
- Kobayashi S, Nakase I, Kawabata N et al (2009) Cytosolic targeting of macromolecules using a pH-dependent fusogenic peptide in combination with cationic liposomes. *Bioconjugate Chem* 20:953–959. <https://doi.org/10.1021/bc800530v>
- Kuehne J, Murphy RM (2001) Synthesis and characterization of membrane-active GALA-OKT9 conjugates. *Bioconjugate Chem* 12:742–749. <https://doi.org/10.1021/bc010001w>
- LeCher JC, Nowak SJ, McMurry JL (2017) Breaking in and busting out: cell-penetrating peptides and the endosomal escape problem. *Biomol Concepts* 8:131–141. <https://doi.org/10.1515/bmc-2017-0023>
- Lee-Huang S, Huang PL, Chen H-C et al (1995) Anti-HIV and anti-tumor activities of recombinant MAP30 from bitter melon. *Gene* 161:151–156. [https://doi.org/10.1016/0378-1119\(95\)00186-a](https://doi.org/10.1016/0378-1119(95)00186-a)
- Li WJ, Nicol F, Szoka FC Jr (2004) GALA: a designed synthetic pH-responsive amphipathic peptide with applications in drug and gene delivery. *Adv Drug Deliv Rev* 56:967–985. <https://doi.org/10.1016/j.addr.2003.10.041>
- Liou JS, Liu BR, Martin AL et al (2012) Protein transduction in human cells is enhanced by cell-penetrating peptides fused with an endosomolytic HA2 sequence. *Peptides* 37:273–284. <https://doi.org/10.1016/j.peptides.2012.07.019>
- Locke T, Sofou S (2017) Clustered versus uniform display of GALA-peptides on carrier nanoparticles: enhancing the permeation of

- noncharged fluid lipid membranes. *Langmuir* 33:13625–13633. <https://doi.org/10.1021/acs.langmuir.7b03706>
- Lonn P, Kacsinta AD, Cui XS et al (2016) Enhancing endosomal escape for intracellular delivery of macromolecular biologic therapeutics. *Sci Rep* 6:32301. <https://doi.org/10.1038/srep32301>
- Luo Z, Cao XW, Li C et al (2016) The heparin-binding domain of HB-EGF as an efficient cell-penetrating peptide for drug delivery. *J Pept Sci* 22:689–699. <https://doi.org/10.1002/psc.2932>
- Martino C, Niccolo T, Massimo S et al (2003) Relative influence of hydrophobicity and net charge in the aggregation of two homologous proteins. *Biochemistry* 42:15078–15083. <https://doi.org/10.1021/bi030135s>
- Meier O, Boucke K, Hammer SV et al (2002) Adenovirus triggers macropinocytosis and endosomal leakage together with its clathrin-mediated uptake. *J Cell Biol* 158:1119–1131. <https://doi.org/10.1083/jcb.200112067>
- Meng Y, Liu S, Li J et al (2012) Preparation of an antitumor and anti-virus agent: chemical modification of alpha-MMC and MAP30 from *Momordica charantia* L. with covalent conjugation of polyethylene glycol. *Int J Nanomed* 7:3133–3142. <https://doi.org/10.2147/IJN.S30631>
- Nakase I, Hirose H, Tanaka G et al (2009) Cell-surface accumulation of flock house virus-derived peptide leads to efficient internalization via macropinocytosis. *Mol Ther* 17:1868–1876. <https://doi.org/10.1038/mt.2009.192>
- Patel SG, Sayers EJ, He L et al (2019) Cell-penetrating peptide sequence and modification dependent uptake and subcellular distribution of green fluorescent protein in different cell lines. *Sci Rep* 9:6298. <https://doi.org/10.1038/s41598-019-42456-8>
- Puri M, Kaur I, Perugini MA et al (2012) Ribosome-inactivating proteins: current status and biomedical applications. *Drug Discov Today* 17:774–783. <https://doi.org/10.1016/j.drudis.2012.03.007>
- Rehman ZU, Hoekstra D, Zuhorn IS (2011) Protein kinase A inhibition modulates the intracellular routing of gene delivery vehicles in HeLa cells, leading to productive transfection. *J Control Release* 156:76–84. <https://doi.org/10.1016/j.jconrel.2011.07.015>
- Roberta AP, Shlomo N et al (1990) Mechanism of leakage of phospholipid vesicle contents induced by the peptide GALA. *Biochemistry* 29:8720–8728. <https://doi.org/10.1021/bi00489a031>
- Rust A, Shah S, Hautbergue G et al (2018) Burkholderia lethal factor 1, a novel anti-cancer toxin, demonstrates selective cytotoxicity in MYCN-amplified neuroblastoma cells. *Toxins (Basel)* 10:261. <https://doi.org/10.3390/toxins10070261>
- Salomone F, Cardarelli F, Di Luca M et al (2012) A novel chimeric cell-penetrating peptide with membrane-disruptive properties for efficient endosomal escape. *J Control Release* 163:293–303. <https://doi.org/10.1016/j.jconrel.2012.09.019>
- Sasaki K, Kogure K, Chaki S et al (2008) An artificial virus-like nano carrier system: enhanced endosomal escape of nanoparticles via synergistic action of pH-sensitive fusogenic peptide derivatives. *Anal Bioanal Chem* 391:2717–2727. <https://doi.org/10.1007/s00216-008-2012-1>
- Shete HK, Prabhu RH, Patravale VB (2014) Endosomal escape: a bottleneck in intracellular delivery. *J Nanosci Nanotechnol* 14:460–474. <https://doi.org/10.1166/jnn.2014.9082>
- Subbarao NK, Parente RA, Szoka FC et al (1987) pH-dependent bilayer destabilization by an amphipathic peptide. *Biochemistry* 26:2964–2972. <https://doi.org/10.1021/bi00385a002>
- Varkouhi AK, Scholte M, Storm G, Haisma HJ (2011) Endosomal escape pathways for delivery of biologicals. *J Control Release* 151:220–228. <https://doi.org/10.1016/j.jconrel.2010.11.004>
- Verdurmen WP, Wallbrecher R, Schmidt S et al (2013) Cell surface clustering of heparan sulfate proteoglycans by amphipathic cell-penetrating peptides does not contribute to uptake. *J Control Release* 170:83–91. <https://doi.org/10.1016/j.jconrel.2013.05.001>
- Wadia JS, Stan RV, Dowdy SF (2004) Transducible TAT-HA fusogenic peptide enhances escape of TAT-fusion proteins after lipid raft macropinocytosis. *Nat Med* 10:310–315. <https://doi.org/10.1038/nm996>
- Walsh MJ, Dodd JE, Hautbergue GM (2013) Ribosome-inactivating proteins: potent poisons and molecular tools. *Virulence* 4:774–784. <https://doi.org/10.4161/viru.26399>
- Wang T, Yang S, Petrenko VA, Torchilin VP (2010a) Cytoplasmic delivery of liposomes into MCF-7 breast cancer cells mediated by cell-specific phage fusion coat protein. *Mol Pharm* 7:1149–1158. <https://doi.org/10.1021/mp1000229>
- Wang W, Nema S, Teagarden D (2010b) Protein aggregation—pathways and influencing factors. *Int J Pharm* 390:89–99. <https://doi.org/10.1016/j.ijpharm.2010.02.025>
- Wiedman G, Fuselier T, He J et al (2014) Highly efficient macromolecule-sized poration of lipid bilayers by a synthetically evolved peptide. *J Am Chem Soc* 136:4724–4731. <https://doi.org/10.1021/ja500462s>
- Wieprecht T, Dathe M, Beyermann M et al (1997) Peptide hydrophobicity controls the activity and selectivity of magainin 2 amide in interaction with membranes. *Biochemistry* 36:6124–6132. <https://doi.org/10.1021/bi9619987>
- Ying T, Kim JS (2008) A fusogenic segment of glycoprotein H from herpes simplex virus enhances transfection efficiency of cationic liposomes. *J Gene Med* 10:646–654. <https://doi.org/10.1002/jgm.1184>
- Zuris JA, Thompson DB, Shu Y et al (2015) Cationic lipid-mediated delivery of proteins enables efficient protein-based genome editing in vitro and in vivo. *Nat Biotechnol* 33:73–80. <https://doi.org/10.1038/nbt.3081>

**Publisher's Note** Springer Nature remains neutral with regard to jurisdictional claims in published maps and institutional affiliations.